Desalination and Water Treatment
www.deswater.com

doi: 10.5004/dwt.2018.21941

108 (2018) 125–135
March

Effect of coagulation and adsorption on DON removal and DBPs formation potential in municipal wastewater effluent

Bing Liu[a,b,*], Li Gu[c], Xingguo Zhang[a,*], Qingfei Li[a], Guozhong Yu[a], Chengmei Zhao[a], Huimin Zhai[a]

[a]*School of Geographic Sciences, Xinyang Normal University, 237 Nanhu Road, Xinyang, 464000, China, Tel. +86 376 6391700; emails: liubing_982002@163.com (B. Liu), xingguozhang@tom.com (X. Zhang), qingfeili1972@163.com (Q. Li), guozhong1966@163.com (G. Yu), zhaocm1971@163.com (C. Zhao), zhaihm8787@163.com (H. Zhai)*
[b]*Institute of Urban Environment, Chinese Academy of Sciences, 1799 Jimei Road, Xiamen 361021, China*
[c]*Key Laboratory of the Three Gorges Reservoir Region's Eco-Environment, Ministry of Education, Chongqing University, 174 Shazheng Street, Chongqing, 400045, China, Tel. +86 23 65127815; email: gu_li1980@163.com*

Received 7 June 2017; Accepted 24 January 2018

ABSTRACT

Municipal wastewater effluent has increasingly been used as reclaimed water and a source of water for downstream communities. Dissolved organic nitrogen (DON) in wastewater effluent can be a precursor of nitrogen disinfection by-products (N-DBPs), which has garnered recent attention. Our results indicated that: (1) the concentration of DON in the effluent was 1.95 mg/L, and the DON was primarily composed of soluble microbial products (SMPs) resulting from the process of biological treatment of sewage. (2) Approximately 20% of the DON could be removed using coagulants at a dosage of 120 mg/L, and almost 80% of the DON was eliminated by adsorption with activated carbon at a dosage of 0.5 g/L. Small molecular weight DON compounds (<6 kDa) comprised most of the DON and accounted for 74.34% of the total. After coagulation, the percent fraction of <6 kDa DON increased, while the fraction of >20 kDa DON decreased. However, adsorption resulted in an opposite trend, with large molecular weight DON increasing and small molecular weight DON decreasing. (3) Hydrophilic and hydrophobic DON comprised most of the DON, and accounted for 58.5% and 30.8% of the DON, respectively. The removal of hydrophilic DON (mean 12%) was lower than that of hydrophobic DON (mean 76%) after coagulation. In contrast, adsorption resulted in a greater removal of hydrophilic DON (mean 83%) than that of hydrophobic DON (mean 49%). (4) Coupling coagulation with adsorption prior to chlorination was the most effective means to lower the formation potential of disinfection by-products (DBPs). The formation potential of monochloro bromoacetonitrile was highest (41.3 μg/L), while that of trichloroacetonitrile was the lowest (1.3 μg/L). (5) Normalized excitation–emission area volumes ($Ø_{i,n}$) were used to quantify 3-DEEM fluorescence. $Ø_{2,n}$ and $Ø_{4,n}$ of fluorescence regions II and IV were highest, and accounted for 23.38% and 46.83% of the total, respectively. SMPs were effectively removed by coagulation or adsorption, which was highlighted by the highest removal rate for $Ø_{4,n}$ compared with the other four $Ø_{i,n}$.

Keywords: Dissolved organic nitrogen; Soluble microbial products; Coagulation; Adsorption; 3-DEEM

1. Introduction

Dissolved organic carbon (DOC), NH_4^+–N, particulate organic nitrogen, and colloidal organic nitrogen (CON) that is present in wastewater treatment plant (WWTP) influent can be removed by various processes and treatments. However, dissolved organic nitrogen (DON) is particularly difficult to eliminate from waste waters [1]. Consequently, the DON concentrations of effluent waters can reach 0.5–3.0 mg/L, which

* Corresponding author.

accounts for 40%–85% of the total dissolved nitrogen (TDN) in effluents [2].

Previous studies have shown that DON in WWTP effluents contain biodegradable DON (BDON) and bioavailable DON (ABDON), which includes free amino acids and urea [3,4]. As much as 28%–57% of DON in secondary effluents from denitrification WWTPs is composed of BDON or ABDON [3]. Others have also reported that BDON and ABDON can account for about 18%–61% of effluent DON [4]. ABDON and BDON that is present in effluent discharge into natural surface waters such as rivers, lakes, and reservoirs, can serve as potential nutrient sources that stimulate algal growth and results in depleted dissolved oxygen (DO) [5,6]. The decreased DO content of natural waters represents a serious threat to water quality. Further, effluent has increasingly been used as reclaimed or drinking water sources for downstream communities. DON is a precursor for nitrogen disinfection by-products (N-DBPs) that can form during chlorination [7–11]. Importantly, the carcinogenic concentration of N-DBPs is much lower than that of carbon disinfection by-products (C-DBPs), suggesting that their formation can pose a particularly acute health risk. For instance, carcinogenic concentrations of dimethyl nitrosamines and diethylnitrosamines are only 0.7 and 0.2 ng/L, respectively [8]. It is, therefore, imperative to minimize DON concentrations in wastewater effluent.

Effluent DOC concentrations can generally be decreased by coagulation, adsorption, ion exchange, advanced oxidation, biodegradation, or other physical and chemical methods [12–16]. Of these, coagulation and adsorption are the most economical and effective means of treatment and are also easily applied in full-scale treatment processes. In contrast to DOC, DON is mainly composed of amino, nitrile, purine, and pyrimidine compounds [17,18], which contain functional groups comprising amine (–NH_2), amide (–CONH–R), nitro (–NO_2), and nitrile (–CN) groups [17,18]. The formation of H-bonding between functional groups and water molecules enhances the hydrophilicity of DON. Previous studies have shown that amino acids with small molecular weight and hydrophilicity can be important components of DON [17,18]. Thus, DON and DOC are distinguished by several properties. Thus, it is critical to investigate the effects of coagulation and adsorption on DON and the formation potential of DBPs in effluent waters.

Here, we investigated the concentrations, molecular weight fractions, and the hydrophobicity/hydrophilicity characteristics of DON in wastewater effluents. The rates of DON removal by coagulation, adsorption, and coupled coagulation–adsorption processing were studied. In addition, the formation potential of DBPs was analyzed after the various treatment processes. Lastly, 3-DEEM was used to further characterize the DON variation among samples.

2. Materials and methods

2.1. Wastewater treatment processes and sampling

This study was carried out at the Xinyang WWTP (4.00×10^4 m^3/d), Xinyang City, Henan Province, China. The treatment processes include grid, primary sedimentation tank, carrousel oxidation ditch, and secondary sedimentation tank. The concentration of solids suspended in mixed liquor in the carrousel oxidation ditch was 2,800 mg/L, and the returned activated sludge was roughly equal to the influent flow. The operating sludge retention time was about 18 d. The effluent was sampled, and then immediately filtered by using 0.45 μm pore size membranes. All filtered samples were stored at 4°C before analysis.

2.2. Analytical methods

DOC was determined using TOC-VCHS analyzer (Shimadzu). UV absorbance at 254 nm (UV_{254}) was determined using a spectrophotometer (752N/UV-2101PC). The special UV absorbance (SUVA) was calculated as UV_{254} divided by mg/L DOC concentration (UV_{254}/DOC), indicating the degree of aromaticity of dissolved organic matter (DOM). NH_4^+–N was measured using salicylate-hypochlorite method. NO_2^-–N was measured using N-(1-naphthyl)-ethylenediamine photometric method. NO_3^-–N was determined using UV spectrophotometry method. TDN, sum of NH_4^+–N, NO_2^-–N, NO_3^-–N, and DON, was measured using alkaline potassium persulfate digestion-UV spectrophotometric method. All the determinations were done according to the Chinese National Standard Methods (SEPA of China [19]). DON was quantified as the difference between TDN and three dissolved inorganic nitrogen species (including NH_4^+–N, NO_3^-–N, and NO_2^-–N). The pH_{PZC} was the corresponding pH value when the zeta potential was 0 mV [20]. The amount of surface groups was determined by Boehm titration method [21]. The surface morphology of the carbon was analyzed using a scanning electron microscopy (SEM, JSM-5600LV). Surface area and pore size distributions for the samples were measured using ASAP2020 surface area analyzer using nitrogen adsorption/desorption method.

DBPs, including trichloroacetonitrile (TCAN), dichloroacetonitrile (DCAN), dichloroacetone (1,1-DCP), trichloronitro methane (TCNM), monochloro bromoacetonitrile (BCAN), trichloroacetone (1,1,1-TCP), dibromoacetonitrile (DBAN), were analyzed after samples being extracted with methyl *tert*-butyl ether (MTBE) using a gas chromatograph (GC-2010, Shimadzu, Japan) equipped with a HP 5 fused silica capillary column (30 m × 0.25 mM i.d., 0.25 μM film thickness, J&W, USA) and an electronic capture detector using the modified USEPA method 551.1. The inlet and detector temperatures were 200°C and 290°C, respectively. The temperature was programmed as follows: the initial holding was at 35°C for 10 min, then increased in rates of 10°C/min to 145°C for 2 min, 2°C/min to 260°C for 5 min. N_2 was used as carrier gas.

2.3. Physical and chemical characteristics of activated carbon

Two types of activated carbon (coconut shell and coal-activated carbon) were cleaned with deionized water at 80°C several times, and then dried at 105°C. Activated carbon with particle sizes of 20–40 mesh were screened, stored, and dried. SEM photographs of the activated carbon are shown in Fig. 1, and the associated physical and chemical parameters are provided in Table 1.

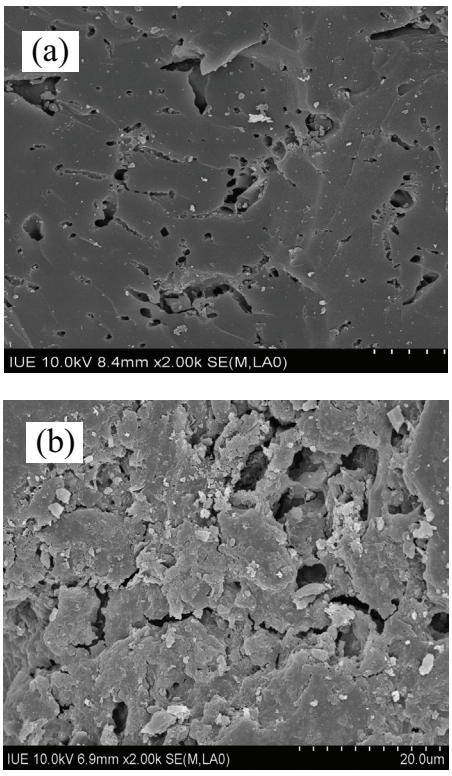

Fig. 1. SEM photographs of two kinds of activated carbon. (a) Coconut shell-activated carbon; (b) Coal-activated carbon.

Table 1
Physical and chemical characteristics of activated carbon used in the analyses

Activated carbon type	Coconut shell	Coal
BET surface area (m^2/g)	973	714
Mean pore diameter (nm)	1.936	2.039
Micropore volume, V_m (cm^3/g)	0.349	0.215
Total pore volume, V_t (cm^3/g)	0.444	0.364
V_m/V_t	0.786	0.591
Basic groups (mmol/g)	0.75	0.70
Acidic groups (mmol/g)	0.78	0.83
pH_{PZC}	6.92	5.43

2.4. Fractionation of molecular weight and hydrophobicity/hydrophilicity

The DON was fractionated by molecular sieves. Two types of regenerated cellulose membranes (Millipore Corp., USA) were used: (1) a membrane with a 20 kDa nominal molecular weight limit (NWML) and (2) a membrane with a 6 kDa NWML. 200 mL of water sample were filtered through the first and second membranes in series. Fifty milliliters of raw water and each filtrate were retained for further analysis. The percentage of DON in each size range was calculated as follows:

$$\%<6\text{k Da}=\frac{C_{6\text{K Permeate}}}{C_{\text{raw}}}\times 100\% \quad (1)$$

$$\%<6\text{k}-20\text{k Da}=\frac{C_{20\text{K Permeate}}-C_{6\text{K Permeate}}}{C_{\text{raw}}}\times 100\% \quad (2)$$

$$\%>20\text{k Da}=\frac{C_{\text{raw}}-C_{20\text{K Permeate}}}{C_{\text{raw}}}\times 100\% \quad (3)$$

where C_i is the measured parameter of fraction i. Thus, we calculated the percentage difference between the measured total mass and the sum of the masses for each mass fraction.

DON in the effluent was separated into three fractions using Amberlite XAD-8, XAD-4 resin by the following procedures. The filtered effluent was acidified to pH 2 using 6 mol/L HCl, and successively passed through the XAD-8, XAD-4 resin column. The eluate from XAD-4 was defined as the hydrophilic DON (HPI), whereas the DOM that remained on the XAD-8 resins was eluted with 0.1 mol/L NaOH at a flow rate of 100 mL/h and collected as the hydrophobic DON (HPO). The transitional DON (TPI) was quantified as the difference between the effluent DON and the sum of HPO and HPI.

2.5. Coagulation tests

Polyaluminium chloride (PACl, 28% Al_2O_3) and aluminum sulfate ($Al_2(SO_4)_3{\cdot}18H_2O$) were used as coagulants in this study. Coagulation was performed using a standard jar tester. The 1 L effluents were placed in beaker at different dosage of 10, 20, 40, 60, 80, 100, and 120 mg/L, and then stirred rapidly for 60 s at 300 rpm, followed by 15 min of slow mixing at 30 rpm and 30 min of settling. The supernatant was taken and filtered through 0.45 μm filter for further analysis. These experiments were conducted without pH adjustments.

2.6. Adsorption tests

Coconut shell and coal-activated carbon were used as adsorbents. Municipal effluent samples (200 mL) were placed in 250 mL Erlenmeyer flasks with different dosages of activated carbon (0.05, 0.1, 0.2, 0.3, 0.4, and 0.5 g/L), and then intensively agitated on a horizontal shaker at 250 rpm and 20°C. After 24 h, the activated carbon was separated from the solution by membrane filtration (0.45 μm pore size) and the remaining sample after adsorption was assessed.

2.7. DBPs formation potential

Seven different kinds of DBPs formation potentials were investigated as well. The pH of the effluent through the 0.45 μm filter was adjusted to 7.0 with 10 mM phosphate buffer solution, and then chlorinated by a certain amount of sodium hypochlorite solution [22]. All chlorinated samples were stored in the dark at room temperature (22°C ± 1°C). After 72 h, the samples were quenched by ascorbic acid, and extracted immediately with MTBE.

2.8. 3DEEM fluorescence spectroscopy

Three-dimensional excitation–emission matrix (3DEEM) fluorescence spectroscopy (F-4600 FL Spectrophotometer,

Hitachi, Japan) was used to characterize dissolved organic matter in water samples. The excitation (Ex) wavelength was set from 200 to 400 nm at 5 nm sampling intervals, corresponding to emission (Em) wavelengths from 280 to 500 nm at the same sampling intervals. The excitation and emission slits were set at 5 nm and the scanning speed was set at 1,200 nm/min. The spectrum of double distilled water was recorded as the blank. The software Origin 7.5 (OriginLab Inc., USA) was employed to process the data. The EEM spectra were plotted as the elliptical shape of contours. The X-axis represented the emission spectra from 280 to 500 nm, and the Y-axis represented excitation from 200 to 400 nm. As a third dimension, a contour line was shown for each EEM spectra to express the fluorescence intensity at an interval of 5 nm. Fluorescence regional integration (FRI) was used for quantification of 3DEEM fluorescence [23].

3. Results and discussion

3.1. Characterization of the effluent

The concentrations of organic and inorganic matter in the effluent are shown in Fig. 2. The TDN concentration of the effluent was 10.26 mg/L while DON was 1.95 mg/L (approximately 20% of the TDN), and NH_4^+–N, NO_3^-–N, NO_2^-–N concentrations were 2.37, 5.86, and 0.08 mg/L, respectively (Fig. 2(a)). DOC concentration was 11.28 mg/L and the ratio of DOC/DON (C/N) was 5.78 mg DOC/mg DON (Fig. 2(b)). UV_{254} and SUVA were 13.23 1/m and 1.17 L/(m mg), respectively (Fig. 2(c)). The molecular weight fractions of DON and DOC in the effluent are shown in Fig. 3. Small molecular weight (<6 kDa) DON accounted for a high proportion of the DON (74.34%), whereas large (>20 kDa) and medium molecular weight (6–20 kDa) DON accounted for 12.21% and 13.45% of the total, respectively (Fig. 3(a)). A bimodal distribution of DOC molecular weight fractionation was observed (Fig. 3(b)). The percentages of large (>20 kDa) and small (<6 kDa) molecular weight fractions were 22.85% and 63.23%, respectively, while the medium molecular weight fraction (6–20 kDa) only accounted for 13.92% of the total DOC.

SUVA is an important index to evaluate the properties of organic matter and is strongly correlated with abundances of aromatic-like organic compounds and unsaturated organic compounds [24]. A SUVA value higher than 4 L/(m mg), indicates a greater concentration of hydrophobic compounds and large molecular weight substances, which would indicate that DOM could be easily removed by coagulation [25]. However, the SUVA value of the effluent analyzed here was only 1.17 L/(m mg), suggesting a lower DOM hydrophobicity which contained the DON. However, the percentage of large molecular weight DON (>20 kDa) was 12.21%. These results suggest that it would be difficult to remove the DON of the effluent analyzed here by coagulation.

Previous studies have shown that the ratio of C/N can be used to identify the origin of organic matter. A lower C/N ratio would indicate that DOM is derived from algae or bacteria, and a higher ratio would suggest that plants or soils contribute more to the DOM pool [26–28]. The ratio of C/N in the effluent was only 5.78 mg DOC/mg DON indicating that the effluent DON was presumably composed of soluble microbial products (SMPs) from the biological treatment of sewage. When microorganisms degrade organic and inorganic matter, SMPs containing large abundances of nitrogen-enriched compounds including proteins, amino acids, polysaccharides, and nucleic acids are released through cell lysis, endogenous cellular respiration, and metabolic losses among other mechanisms [29]. Thus, others have argued that DON could be a proxy for SMP production [30].

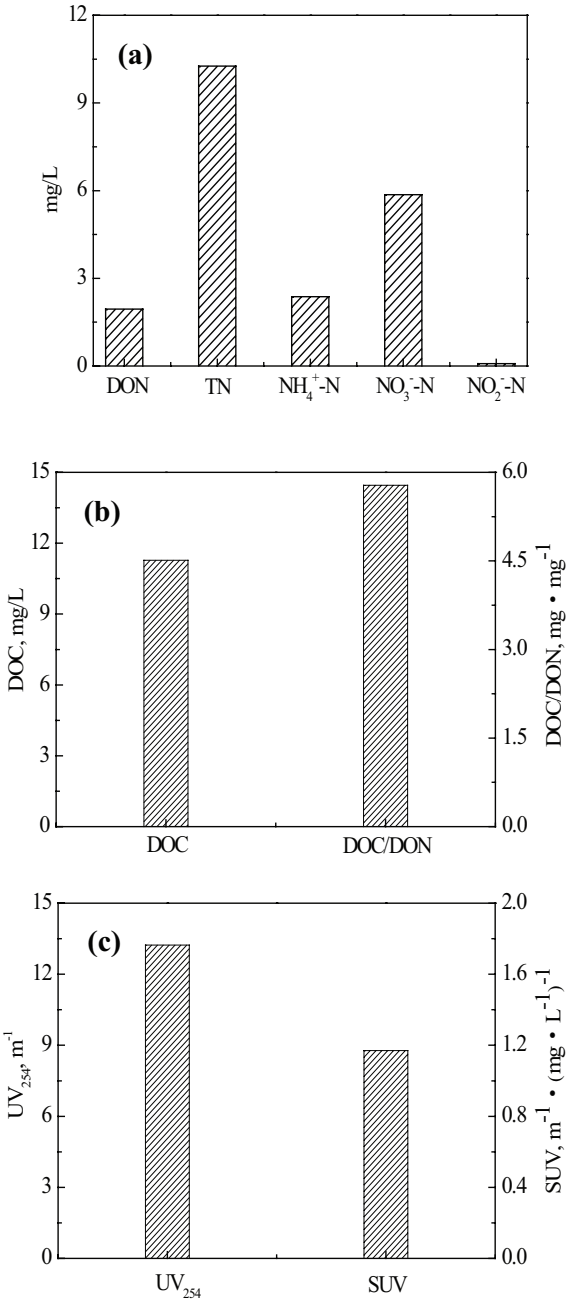

Fig. 2. Characterization of the effluent. (a) DON, TDN, NH_4^+–N, NO_3^-–N, NO_2^-–N concentrations; (b) DOC concentration and ratio of N/C; (c) UV_{254} and SUVA. Data are averages of three replicate analyses, and all relative standard deviations (n = 3) were below 9%.

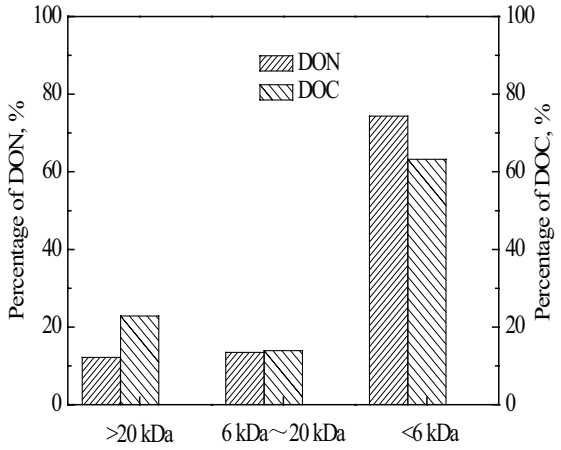

Fig. 3. Molecular weight fractionation of DON and DOC in municipal wastewater effluent. (a) DON, (b) DOC. Data are averages of three replicates, and their relative standard deviations (n = 3) were all below 6%.

3.2. DON, DOC, and UV_{254} coagulation analyses

The removal of DON, DOC, and UV_{254} by coagulation with increasing PAC1 and aluminum sulfate dosages were evaluated and the results are shown in Fig. 4. The removal of DON, DOC, and UV_{254} with increasing coagulant dosage followed similar trends. The rate of DON removal reached 18.08% and 16.37% at dosages of 120 mg/L of both PAC1 and aluminum sulfate (Fig. 4(a)). At the same dosage, the rates of DOC removal were 26.97% and 24.78%, respectively, and the efficiencies of UV_{254} removal were 45.58% and 43.32%, respectively. The removal efficiency for the surrogate parameters followed the order of: UV_{254} > DOC > DON. A greater removal rate of UV_{254} compared with that of DOC and DON is consistent with previous studies [31].

Coagulants are mainly used to remove suspended particles and colloidal substances from waters [32]. However, they can also be applied as an effective method for the removal of DOM [33]. Previous reports have shown that flocculants that form during hydrolysis exhibit positive charges, and could adsorb negatively charged DOM [33]. The DOM that is removed can include high abundances of nitrogenous functional groups, which aids in the removal of about 20% of DON using coagulation. Here, the rate of DOC removal was slightly higher than that of DON removal, which may be related to the distribution of different molecular weight fractions (Fig. 3).

The rates of DON, DOC, and UV_{254} removal after PACl coagulation were slightly higher than what was observed with aluminum sulfate. These results could be explained by several observations. First, the overall charge value of PACl is much higher than that of aluminum sulfate, which could lead to a stronger neutralizing ability of PACl [34]. Second, PACl has a larger molecular weight, and its long chain structure could enhance bridging and netting [34]. When the coagulant dosage was below 60 mg/L, PACl had a considerably greater removal rate of DON (1.3×) compared with aluminum sulfate, and was generally more effective than aluminum sulfate, regardless of dosage (Fig. 3). Therefore, the neutralization mechanism may be particularly dominant at low dosages of coagulant.

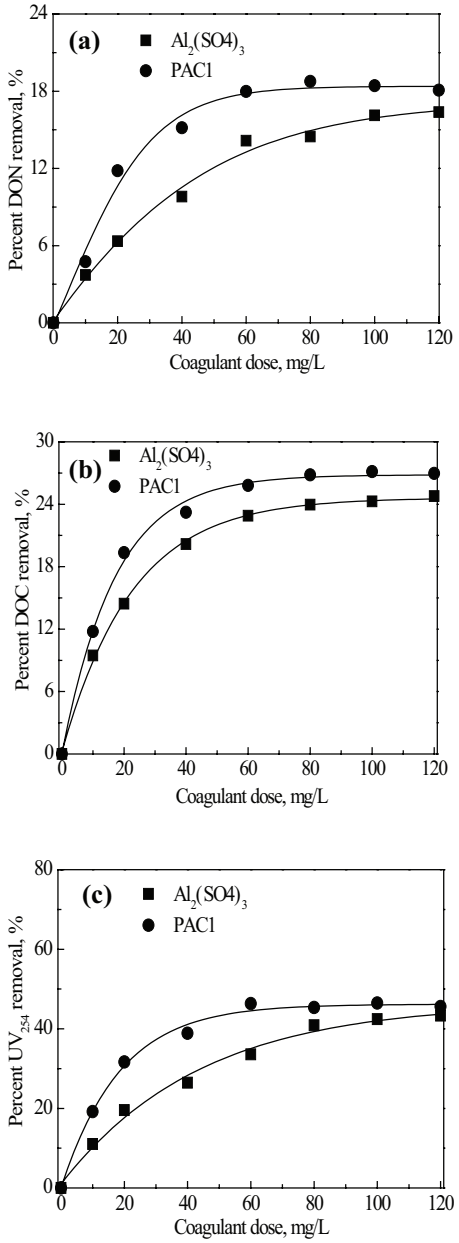

Fig. 4. Percent DON, DOC, and UV_{254} removal after coagulation with increasing aluminum sulfate and PACl doses. (a) Percent DON removal, (b) Percent DOC removal, (c) Percent UV_{254} removal. Data are averages of three replicates, and all standard deviations (n = 3) were below 8%.

3.3. DON, DOC, and UV_{254} adsorption performance studies

The removal efficiency of DON, DOC, and UV_{254} by activated carbon adsorption is shown in Fig. 5. With increasing activated carbon dosages, the rate of DON removal increased (Fig. 5(a)). At activated carbon dosages of 0.5 g/L, the rates of DON removal reached 80.96% and 71.86% for coal and coconut shell-activated carbon, respectively. In addition, the rate of DON removal increased fastest at dosages ranging from 0.05 to 0.2 g/L, regardless of which type of activated carbon was used.

DOC and UV_{254} removal profiles were similar to that of DON (Figs. 5(b) and (c)). At activated carbon dosages of 0.5 g/L, the rates of DOC removal were 53.54% and 46.87% for coal and coconut shell-activated carbon, respectively. Compared with DON and DOC, UV_{254} was eliminated significantly more, with removal rates approaching 90.98% and 79.72%. UV_{254} has been reported to reflect abundances of aromatic-like compounds containing C=C and C=O double bonds. Consequently, adsorption is more effective for removing aromatic-like compounds [35]. These observations likely explain why the rate of UV_{254} removal was higher than that of DON and DOC. The adsorption isotherm of DON is shown in Fig. 5(d), and was fitted using the Freundlich isotherm model. Isotherm constants and correlation coefficients are provided in Table 2. Adsorption isotherm experiments were conducted to investigate the DON adsorption capacity of different activated carbon treatments.

The removal efficiencies of DON, DOC, and UV_{254} via adsorption with coconut shell-activated carbon were much higher than by activated coal carbon (Fig. 5 and Table 2). This difference could be explained by a number of mechanisms: (1) the adsorption capacity of activated carbon is closely related to its pore structure [36]. Generally, the pore structure of activated carbon should match the molecular dimensions of DOM. As shown in Fig. 3(a), small molecular weight (<6 kDa) DON was the dominant DON fraction in the effluent. In addition, physical analyses indicated that the specific surface area, micropore volume, and ratio of micropore to total pore of coconut shell-activated carbon were relatively higher than the coal-activated carbon (Table 1), which likely resulted in greater adsorption of small molecular weight DON. (2) The surface of coal-activated carbon possessed higher concentrations of acidic groups and exhibited stronger hydrophilicity

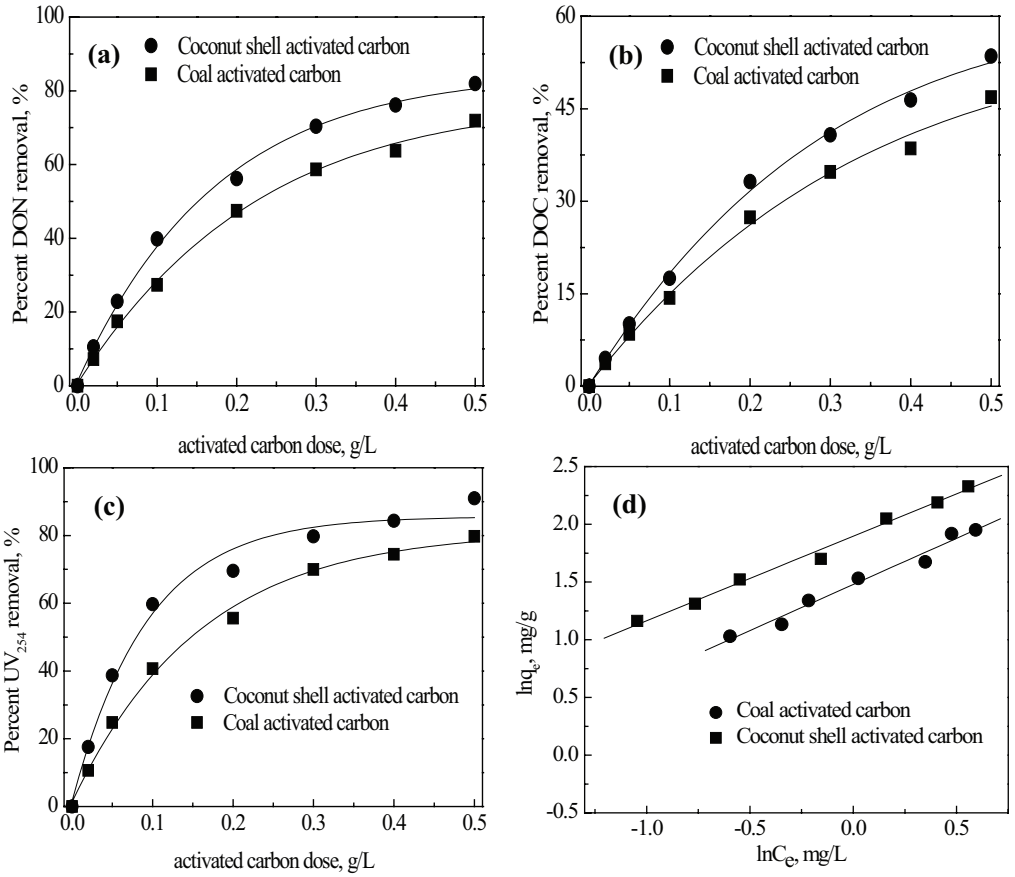

Fig. 5. Percent DON, DOC, and UV_{254} removal after adsorption using activated carbon. (a) Percent DON removal; (b) Percent DOC removal; (c) Percent UV_{254} removal; (d) DON adsorption isotherm. Data are averages of three replicates and their relative standard deviations (n = 3) were all below 7%.

Table 2
Parameters of the DON adsorption isotherm

	Freundlich isotherm			Langmuir isotherm		
	K_f(mg/g)/(mg/L)^n	1/n	R^2	q_{max}(mg/g)	b (L/mg)	R^2
Coconut shell-activated carbon	6.667	0.733	0.969	27.639	0.328	0.985
Coal-activated carbon	4.386	0.798	0.977	25.829	0.206	0.966

(Table 1) [36]. Based on a π–π dispersion mechanism [37], water molecules would form strong H-bonds with the hydrophilic functional groups of the coal-activated carbon surface, which would hinder the adsorption of DON molecules. The competition for adsorption between water molecules and DON would then weaken the adsorption effect of DON with coal-activated carbon surfaces. (3) The pH_{PZC} value of the surface of coal-activated carbon was 5.43 (Table 1), indicating that it contained a greater abundance of negative charges. Thus, charge rejection between the surface of coal-activated carbon and the negative charges of DOM would result in weaker adsorption [37,38]. The surface of coconut shell-activated carbon contained higher positive charge and it would be easier to form electron donor–acceptor complexes with negatively charged DOM via the mechanism of electron donor–acceptor complexes [38], which would then result in greater DON removal. (4) Effluent DON was mainly composed of tryptophan protein-like substances, aromatic protein-like substances and fulvic acids-like substances, such as tryptophan acid and fulvic acid (Fig. 9). The higher concentration of basic groups on the coconut shell-activated carbon surface would lead to greater reactivity with the acidic functional groups of tryptophan acid and fulvic acid, among other acidic-group containing complexes.

3.4. Removal of DON and DOC by coupling coagulation with adsorption

The effluent was first treated by coagulation at a dosage of 60 mg/L, and then adsorption with activated carbon at a dosage of 0.1 g/L. The percentages of DON and DOC that were removed using this coupled coagulation and adsorption methodology are shown in Fig. 6. The maximum removal rates of DON and DOC were 69.15% and 58.24%, respectively. The original concentrations of DON and DOC in the effluent were 1.95 and 11.28 mg/L, respectively, but were reduced to 0.60 and 4.71 mg/L, respectively, after treatment with coupled coagulation with adsorption. Moreover, the formation potential of DBPs was also greatly decreased (Fig. 8). Importantly, the rate of DON removal by coupling coagulation and adsorption was higher than the sum of individual coagulation and adsorption treatments. This increase in removal could likely be explained by either of two mechanisms: (1) large molecular weight DON was removed by coagulation, and the small molecular weight fraction was then eliminated by adsorption resulting in overall greater DON removal. (2) Activated carbon micropores that were blocked by organic matter declined in abundance after coagulation, and the adsorption capacity of smaller molecular weight organic matter then increased [39,40]. Regardless of the exact mechanism, the rates of DON and DOC removal were enhanced by coupling coagulation with adsorption to treat wastewater effluent.

3.5. Molecular weight fractionation and hydrophobicity/hydrophilicity of DON

Molecular weight fractions of DON are shown in Fig. 7(a) for sample 1 (the effluent), sample 2 (treated with coagulation at a dosage of 60 mg/L), sample 3 (treated by adsorption with coconut shell-activated carbon at a dosage of 0.1 g/L),

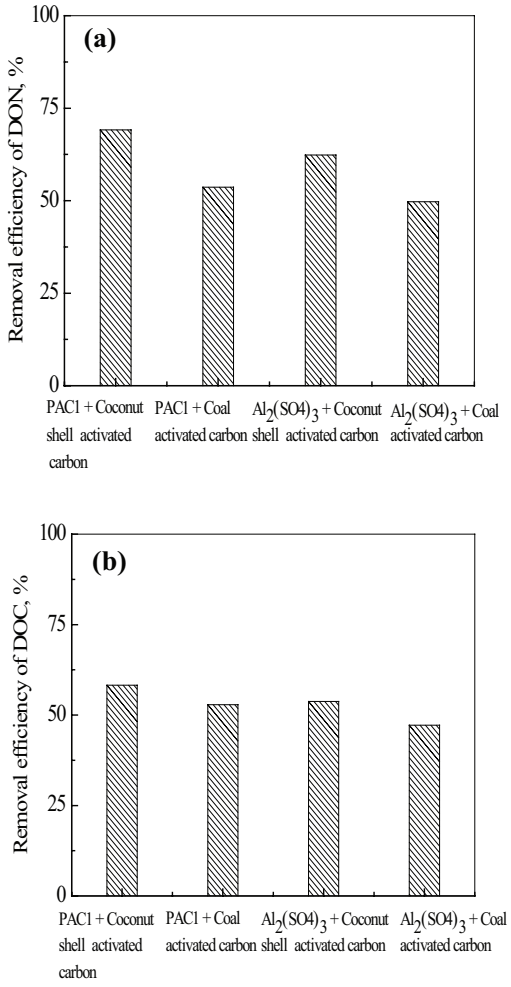

Fig. 6. Removal efficiencies of DON and DOC after coagulation combined with adsorption (coagulant dosage = 60 mg/L; activated carbon dosage = 0.1 g/L). (a) DON removal efficiency; (b) DOC removal efficiency. Data are averages of three replicates and all relative standard deviations (n = 3) were below 9%.

and sample 4 (coagulation with a PACl dosage of 60 mg/L and adsorption with a coconut shell-activated carbon dosage of 0.1 g/L). The small (<6 kDa) and middle (6–20 kDa) molecular weight fractions accounted for 74.34% and 13.45% of the DON, respectively, while the large molecular weight DON (>20 kDa) only accounted for about 12.21% of the total DON. After coagulation, the fraction of <6 kDa DON increased from 74.34% to 78.76%, while the fraction of >20 kDa decreased from 12.21% to 9.09%. The molecular weight fraction in the range of 6–20 kDa was roughly equivalent before and after coagulation, comprising DON percentages of 13.45% and 12.15%, respectively. The removal of large molecular weight (>20 kDa) DON was higher after coagulation. After adsorption treatment, the fraction of DON belonging to the molecular weight class of <6 kDa exhibited a decrease from 71.34% to 53.89%, while >20 kDa DON increased from 12.21% to 28.32% of total DON. For the DON fraction in the 6–20 kDa range, adsorption resulted in a moderate increase from 13.45% to 17.77% of total DON. Thus, the removal of small molecular weight (<6 kDa) DON was particularly prevalent

after adsorption. Differences in molecular weight fraction after coupling coagulation with adsorption exhibited similar results as compared with adsorption alone.

The variation in hydrophobicity/hydrophilicity after different treatment processes is shown in Fig. 7(b). Hydrophilic and hydrophobic DON were clearly dominant in the effluent, accounting for 58.5% and 30.8% of the total, respectively. The rate of hydrophilic DON removal by coagulation (mean 12%) was lower than that of hydrophobic DON removal (mean 76%), which led to an increase of hydrophilic DON from 58.5% to 71.4% of the total and a decrease in hydrophobic DON from 30.8% to 12.3% of the total. Thus, coagulation was more effective in the removal of hydrophobic large molecular weight DON. In contrast, adsorption resulted in a higher hydrophilic DON removal rate (mean 83%) compared with hydrophobic DON removal (mean 49%) corresponding to a decrease of total DON from 58.5% to 41.8% for hydrophilic DON and an increase from 30.8% to 32.7% for hydrophobic DON. Thus, hydrophilic small molecular weight DON was more effectively removed by adsorption. The differences in hydrophobicity/hydrophilicity of DON after coupling coagulation with adsorption were similar to what was observed after adsorption alone.

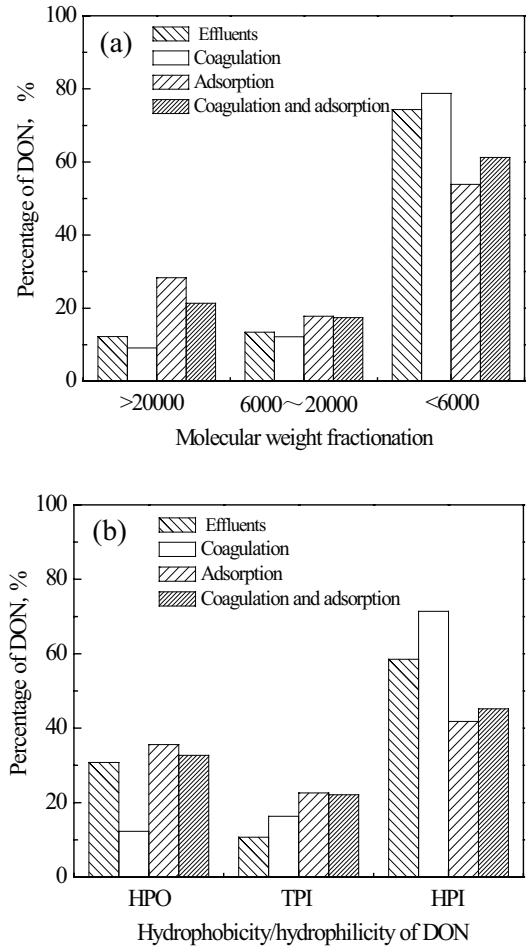

Fig. 7. Molecular weight fractionation and hydrophobicity/hydrophilicity of DON. Data are averages of three replicates, and their relative standard deviations (n = 3) were all below 10%.

3.6. DBP formation potentials

Formation potentials for DBPs resulting from chlorination of the samples were investigated and are shown in Fig. 8. During chlorination of the effluent (sample 1), the formation potential of BCAN was the highest (41.3 μg/L). Due to base-catalyzed hydrolysis at pH > 5.5 [41], the formation potential of TCAN was minimal, and only reached 1.3 μg/L. Previous studies have shown that the formation potentials of some DBPs are reduced as DON concentration decreases [11,41]. All seven types of DBP formation potentials that were assessed decreased after different treatment processes. Hydrophilic, low-molecular weight DON is thought to be a precursor to TCNM [42], and is poorly removed by coagulation, which may explain why TCNM concentration remained almost unchanged in sample 2 after treatment. SMPs (e.g., nucleic acids, proteins, amino acids) are positively correlated with BCAN, DCAN, DBAN, and TCAN yields during chlorination [42]. SMPs were effectively eliminated from the effluent by coagulation, adsorption, and by coupling coagulation with adsorption (Fig. 9). Thus, the formation potentials of BCAN, DCAN, DBAN, and TCAN all decreased after treatment here. Consequently, coupling coagulation with adsorption was the most effective means for lowering formation potentials of all DBPs in this study.

3.7. Characterization of DON

3-DEEM had been widely used to characterize DOM [43], and a good linear relationship between peak intensity of 3-DEEM spectra and DON concentration has been reported [44–46]. As shown above, coupling coagulation with adsorption had a substantial effect on the variation of DON characteristics. 3-DEEM was used to further characterize DON variation among the various treatment strategies (Fig. 9). Using consistent excitation and emission wavelength boundaries for each 3-DEEM spectra, horizontal and vertical lines were drawn to divide the 3-DEEM spectra into five regions. 3-DEEM peaks were associated with humic-like, tyrosine-like, tryptophan-like, and phenol-like organic compounds [23]. Regions I and II were located at the excitation/emission (Ex/Em) wavelengths of 200–250/280–320 nm and 200–250/320–380 nm, respectively, and are associated with simple aromatic protein-like

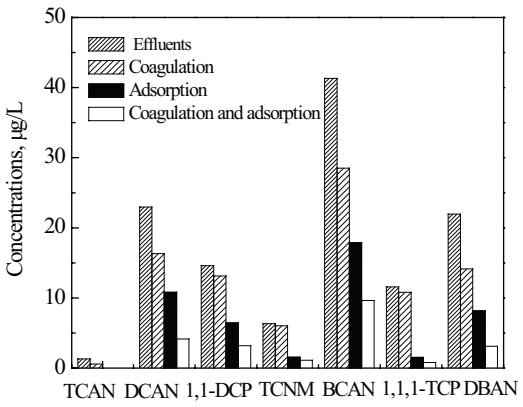

Fig. 8. Formation potentials of chlorination disinfection by-products. Data are averages of three replicates, and their relative standard deviations (n = 3) were all below 8%.

substances such as tyrosine. Region III was located at the excitation/emission (Ex/Em) wavelengths of 200–250/380–500 nm, and is related to fulvic acid-like materials. Region IV was located at the excitation/emission (Ex/Em) wavelengths of 250–280/280–380 nm, and represents SMPs, such as tryptophan protein-like substances. Region V was present at the excitation/emission (Ex/Em) wavelengths of 250–400/380–500 nm, and is related to humic acid-like organics.

FRI was used for further quantification of 3-DEEM fluorescence. $Ø_{i,n}$ of different 3-DEEM regions were calculated and are summarized in Table 3. $Ø_{i,n}$ represents the relative organic matter content of different regions [23]. The $Ø_{i,n}$ of fluorescence regions I, II, III, IV, and V in the effluent were 3.13, 11.26, 5.08, 22.56, and 6.14 (10^5 au nm^2), respectively (Table 3). The $Ø_{2,n}$ and $Ø_{4,n}$ of fluorescence regions II and IV were largest, and accounted for 23.38% and 46.83% of the total, which indicated that effluent DOM was primarily composed of SMPs and aromatic protein-like substances. After coagulation (sample b), the $Ø_{i,n}$ of fluorescence regions I, II, III, IV, and V decreased. However, the rate of removal of $Ø_{4,n}$ in region IV was the highest, and comprised 42.06% of the total. SMPs consist of molecules such as tryptophan, tyrosine, polysaccharides, and nucleic acids, which contain amino, carboxyl, hydroxyl, sulfonic acid, and phenolic

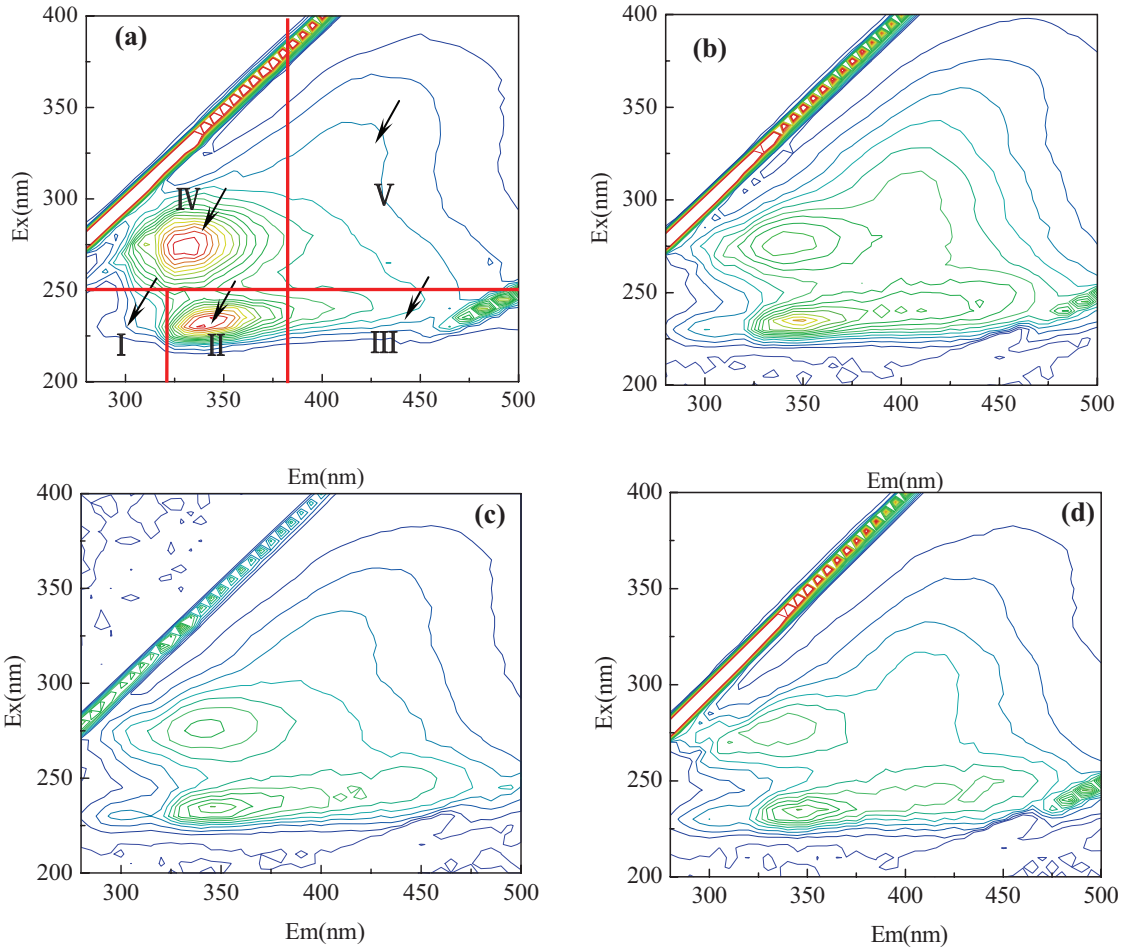

Fig. 9. 3-DEEM spectra of different water samples. (a) Effluents; (b) coagulation-treated; (c) adsorption-treated; (d) coagulation and adsorption treated.

Table 3
FRI parameters of different samples

Samples	Region I	Region II	Region III	Region IV	Region V
	$Ø_{1,n}/10^5$·au·nm^2	$Ø_{2,n}/10^5$·au·nm^2	$Ø_{3,n}/10^5$·au·nm^2	$Ø_{4,n}/10^5$·au·nm^2	$Ø_{5,n}/10^5$·au·nm^2
a	3.13	11.26	5.08	22.56	6.14
b	2.23	9.34	4.76	13.07	5.93
c	2.28	8.13	3.79	10.24	5.21
d	2.16	7.97	4.64	7.62	5.68

hydroxyl functional groups. It is likely that complexing reactions occurred between SMPs and polyvalent metal ions (e.g., Cu^{2+}, Al^{3+}, Fe^{3+}) to form organic-metal compounds [47]. Consequently, the higher concentrations of Al^{3+} from PACl coagulation promoted complexation reactions, which ultimately resulted in the removal of SMPs. During adsorption (sample c), the rate of removal of $Ø_{4,n}$ in region IV was the highest, and approached 54.61%, suggesting that adsorption using activated carbon was the most effective way to eliminate SMPs from the effluent [48]. Coagulation with adsorption significantly lowered the $Ø_{i,n}$ of 3-DEEM regions (sample d), which is consistent with the removal of DON and the lowering of DBP formation potentials.

4. Conclusions

(1) The concentration of DON was 1.95 mg/L in the effluent, and the DOC/DON ratio was 5.78 mg DOC/mg DON. Small molecular weight (<6 kDa) DON accounted for most of the DON (74.34% of the total). Analyses indicated that the DON was primarily composed of SMPs resulting from the process of biological treatment of sewage.

(2) The rate of DON removal reached 18.08% and 16.37% at dosages of 120 mg/L PAC1 and aluminum sulfate, respectively. Increasing activated carbon dosages resulted in increasing DON removal rates. The rates of DON removal reached 80.96% and 71.86% using an activated carbon dosage of 0.5 g/L of coconut shell and coal-activated carbon, respectively. The rate of DON removal when coupling coagulation with adsorption was higher than the sum of individual coagulation and adsorption treatment processing.

(3) After coagulation, the small weight fraction (<6 kDa) of DON increased, while the large weight fraction (>20 kDa) of DON decreased. However, adsorption resulted in an opposite trend, showing an increase in the larger DON weight fraction. Hydrophilic and hydrophobic DON accounted for most of the DON in the effluent, comprising 58.5% and 30.8% of the total, respectively. The rate of hydrophilic DON removal (mean 12%) was lower than that of hydrophobic DON (mean 76%) after coagulation treatment. In contrast, the rate of hydrophilic DON removal (mean 83%) was higher than that of hydrophobic DON (mean 49%) when treating with adsorption.

(4) The formation potential of BCAN in the effluent (41.3 μg/L) was the highest of seven types of DBPs, while TCAN formation potential was the lowest (1.3 μg/L). However, all seven types of DBP formation potentials that were assessed, decreased with the different treatment processes. Coupling coagulation with adsorption was the most effective means to lower the formation potentials of all DBPs that were assessed.

(5) The $Ø_{i,n}$ of fluorescence regions I, II, III, IV, and V in the effluent were 3.13, 11.26, 5.08, 22.56, and 6.14 (10^5 au nm^2), respectively. The $Ø_{2,n}$ and $Ø_{4,n}$ of fluorescence regions II and IV were the highest, and accounted for 23.38% and 46.83% of the total, respectively. The rate of $Ø_{4,n}$ removal in region IV was the highest of any $Ø_{i,n}$ under different treatment processes. The results thus suggested that SMPs were effectively eliminated by coagulation or adsorption.

Acknowledgements

The authors would like to acknowledge the financial support for this work provided by National Natural Science Foundation of China (NSFC) (No. 51208448), Henan Provincial Science and Technology Project (No. 162102310498), Young teacher support program of Henan colleges and universities (No. 2015GGJS-136), the Key Program of Henan Educational Committee (No. 14A610004), and Nanhu Scholars Program for Young Scholars of XYNU.

References

[1] J. Mekinia, H.D. Stensel, K. Czerwionka, J. Drewnowski, D. Zapero, Nitrogen transformations and mass balances in anaerobic/anoxic/aerobic batch experiments with full-scale biomasses from BNR activated sludge systems, Water Sci. Technol., 60 (2009) 2463–2470.

[2] K.R. Pagilla, M. Urgun-Demirtas, R. Ramani, Low effluent nutrient treatment technologies for wastewater treatment, Water Sci. Technol., 53 (2006) 165–172.

[3] C. Sattayatewa, K. Pagilla, P. Pitt, K. Selock, T. Bruton, Organic nitrogen transformations in a 4-stage Bardenpho nitrogen removal plant and bioavailability/biodegradability of effluent DON, Water Res., 43 (2009) 4507–4516.

[4] E. Pehlivanoglu, D.L. Sedlak, Bioavailability of wastewater derived organic nitrogen to the alga *Selenastrum capricornutum*, Water Res., 38 (2004) 3189–3196.

[5] P. Glibert, C.A. Heil, D.J. Hollander, M. Revilla, A. Hoare, J. Alexander, S. Murasko, Evidence for dissolved organic nitrogen and phosphorus uptake during a *cyanobacterial* bloom in Florida Bay, Mar. Ecol. Prog. Ser., 280 (2004) 73–83.

[6] L.L. Bai, C.C. Cao, C.H. Wang, H.C. Xu, H. Zhang, V. Slaveykova, H.L. Jiang, Toward quantitative understanding of the bioavailability of dissolved organic matter in freshwater lake during *cyanobacteria* blooming, Environ. Sci. Technol., 51 (2017) 6018–6026.

[7] G.A. de Vera, W. Gernjak, H. Weinberg, M.J. Farré, J. Keller, U. von Gunten, Kinetics and mechanisms of nitrate and ammonium formation during ozonation of dissolved organic nitrogen, Water Res., 108 (2017) 451–461.

[8] K. Hohner, K. Cawley, J. Oropeza, R.S. Summers, F.L. Rosario-Ortiz, Drinking water treatment response following a Colorado wildfire, Water Res., 105 (2016) 187–198.

[9] W.H. Chu, D.M. Li, Y. Deng, N.Y. Gao, Y.S. Zhang, Y.P. Zhu, Effects of UV/PS and UV/H_2O_2 pre-oxidations on the formation of trihalomethanes and haloacetonitriles during chlorination and chloramination of free amino acids and short oligopeptides, Chem. Eng. J., 301 (2016) 65–72.

[10] Y.H. Chuang, H.H. Tung, Formation of trichloronitromethane and dichloroacetonitrile in natural waters: precursor characterization, kinetics and interpretation, J. Hazard. Mater., 283 (2015) 218–226.

[11] S.W. Krasner, W.A. Mitch, D.L. McCurry, D. Hanigan, P. Westerhoff, Formation, precursors, control, and occurrence of nitrosamines in drinking water: a review, Water Res., 47 (2013) 4433–4450.

[12] X.L. Shi, C.H. Xu, H. Hu, F. Tang, L. Sun, Characterization of dissolved organic matter in the secondary effluent of pulp and paper mill wastewater before and after coagulation treatment, Water Sci. Technol., 74 (2016) 1346–1353.

[13] M. Umar, F. Ruddick, L. Fan, Comparison of coagulation efficiency of aluminum and ferric-based coagulants as pre-treatment for UVC/H_2O_2 treatment of wastewater RO concentrate, Chem. Eng. J., 284 (2016) 841–849.

[14] B.K. Pramanik, F.A. Roddick, L. Fan, A comparative study of biological activated carbon, granular activated carbon and coagulation feed pre-treatment for improving micro-filtration performance in wastewater reclamation, J. Membr. Sci., 475 (2015) 147–155.

[15] S. Xue, W. Jin, Z. Zhang, H. Liu, Reductions of dissolved organic matter and disinfection by-product precursors in full-scale wastewater treatment plants in winter, Chemosphere, 179 (2017) 395–404.
[16] F. Zietzschmann, C. Stutzer, M. Jekel, Granular activated carbon adsorption of organic micro-pollutants in drinking water and treated wastewater-Aligning breakthrough curves and capacities, Water Res., 92 (2016) 180–187.
[17] Y.Y. Zhao, J. Boyd, S.E. Hrudey, X.F. Li, Characterization of new nitrosamines in drinking water using liquid chromatography and mass spectrometry, Environ. Sci. Technol., 40 (2006) 7636–7641.
[18] T. Wadhawan, H. Simsek, M. Kasi, K. Knutson, B. Prüβ, J. McEvoy, E. Khan, Dissolved organic nitrogen and its biodegradable portion in a water treatment plant with ozone oxidation, Water Res., 54 (2014) 318–326.
[19] SEPA of China, Water and Wastewater Monitoring Methods, China Environmental Science Publishing House, Beijing, 2002.
[20] L. Li, S.Q. Liu, J.X. Liu, Surface modification of coconut shell based activated carbon for the improvement of hydrophobic VOC removal, J. Hazard. Mater., 192 (2011) 683–690.
[21] H. Boehm, Surface oxides on carbon and their analysis: a critical assessment, Carbon, 40 (2002) 145–149.
[22] H. Jia, S. Hocheol, W.A. Jesse, T. Karanfil, Halonitromethane formation potentials in drinking waters, Water Res., 44 (2010) 105–114.
[23] W. Chen, P. Westerhoff, J.A. Leenheer, K. Booksh, Fluorescence excitation-emission matrix regional integration to quantify spectra for dissolved organic matter, Environ. Sci. Technol., 37 (2003) 5701–5710.
[24] J.L. Weishaar, G.R. Aiken, B.A. Bergamaschi, M.S. Fram, R. Fujii, K. Mopper, Evaluation of specific ultra-violet absorbance as an indicator of the chemical composition and reactivity of dissolved organic carbon, Environ. Sci. Technol., 37 (2003) 4702–4708.
[25] J.K. Edzwald, J.E. Van Benschoten, Aluminum Coagulation of Natural Organic Matter, Chemical Water and Wastewater Treatment, Springer-Verlag, Berlin, 1990.
[26] P. Westerhoff, H. Mash, Dissolved organic nitrogen in drinking water supplies: a review, J. Water Supply. Res. Technol., 51 (2002) 415–448.
[27] E.M. Thurman, Organic Geochemistry of Natural Waters, Kluwer Academic Publishers, Netherlands, 1985.
[28] G. Aiken. E. Cotsaris, Soil and hydrology: their effect on NOM, J. Am. Water Works Assoc., 87 (1995) 36–45.
[29] B. Liu, L. Gu, X. Yu, G.Z. Yu, C.M. Zhao, Q.F. Li, H.M. Zhai, Profile of dissolved organic nitrogen (DON) in full-scale ozone and biological activated carbon filter, Desal. Wat. Treat., 55 (2015) 2069–2078.
[30] S.N. Nam, G. Amy, Differentiation of wastewater effluent organic matter (EfOM) from natural organic matter (NOM) using multiple analytical techniques, Water Sci. Technol., 57 (2008) 1009–1015.
[31] I. Garcia, L. Moreno, Removal of nitrogen and carbon organic matter by chitosan and aluminium sulphate, Water Sci. Technol. Water Supply, 12 (2012) 1–10.
[32] H. Xu, C. Yang, H. Jiang, Aggregation kinetics of inorganic colloids in eutrophic shallow lakes: influence of cyanobacterial extracellular polymeric substances and electrolyte cations, Water Res., 106 (2016) 344–351.
[33] Y.X. Zhou, M.Q. Yan, R.P. Liu, D.S. Wang, J.H. Qu, Investigating the effect of hardness cations on coagulation: the aspect of neutralisation through Al(III)-dissolved organic matter (DOM) binding, Water Res., 115 (2017) 22–28.
[34] G. Lu, C.L. Li, Y.G. Zheng, A.H. Deng, Effect of different coagulants on the ultraviolet light intensity attenuation, Desal. Wat. Treat., 37 (2012) 302–307.
[35] J.L. Acero, F.J. Benitez, F.J. Real, F. Teva, Micropollutants removal from retentates generated in ultrafiltration and nanofiltration treatments of municipal secondary effluents by means of coagulation, oxidation, and adsorption processes, Chem. Eng. J., 289 (2016) 48–58.
[36] A.D. Seyed, K. Tanju, W. Cheng, Tailoring activated carbons for enhanced removal of natural organic matter from natural waters, Carbon, 42 (2004) 547–557.
[37] E.A. Muller, F.R. Hung, K.E. Gbbbins, Adsorption of water vapor-methane mixtures on activated carbons, Langmuir, 16 (2000) 5418–5424.
[38] C. Moreno-Castilla, J. Rivera-Utrilla, M.V. Lopez-Ramon, F. Carrasco-Marín, Adsorption of some substituted phenols on activated carbons from a bituminous coal, Carbon, 33 (1995) 845–851.
[39] F. Plourde-Lescelleur, I. Papineau, A. Carrière, A. Gadbois, B. Barbeau, NOM removal: evaluating five process alternatives to alum coagulation, J. Water Supply. Res. Technol., 64 (2015) 278–289.
[40] J.L. Acero, F.J. Benitez, Coupling of adsorption, coagulation, and ultrafiltration processes for the removal of emerging contaminants in a secondary effluent, Chem. Eng. J., 210 (2012) 1–8.
[41] J.P. Crou e, D.A. Reckhow, Destruction of chlorination byproducts with sulfite, Environ. Sci. Technol., 23 (1989) 1412–1419.
[42] G.A. de Vera, J. Keller, W. Gernjak, H. Weinberg, M.J. Farré, Biodegradability of DBP precursors after drinking water ozonation, Water Res., 106 (2016) 550–561.
[43] R.K. Henderson, A. Baker, K.R. Murphy, K.R. Murphy, A. Hambly, R.M. Stuetz, S.J. Khan, Fluorescence as a potential monitoring tool for recycled water systems: a review, Water Res., 43 (2009) 863–881.
[44] B. Liu, L. Gu, X. Yu, G.Z. Yu, H.N. Zhang, J.L. Xu, Dissolved organic nitrogen (DON) profile during backwashing cycle of drinking water bio-filtration, Sci. Total. Environ., 414 (2012) 508–514.
[45] B. Liu, L. Gu, X. Yu, H.N. Zhang, Dissolved organic nitrogen (DON) in a full-scale drinking water treatment plant, J. Water Supply. Res. Technol., 61 (2012) 41–49.
[46] E. Pehlivanoglu-Mantas, D.L. Sedlak, Wastewater-derived dissolved organic nitrogen: analytical methods, characterization, and effect-a review, Crit. Rev. Environ. Sci. Technol., 36 (2006) 26–85.
[47] J. Xu, H.W. Luo, Y.K. Wang, G.P. Sheng, Fluorescence approach for investigating binding properties between metals and soluble microbial products from a biological wastewater treatment plant, Process. Biochem., 50 (2015) 636–642.
[48] M.M. Wang, Y.J. Meng, D.F. Ma, Y. Wang, F.L. Li, X. Xu, C.F. Xia, B.Y. Gao, Integration of coagulation and adsorption for removal of N-nitrosodimethylamine (NDMA) precursors from biologically treated municipal wastewater, Environ. Sci. Pollut. Res. Int., 24 (2017) 12426–12436.